Development/Plasticity/Repair

Adult Neurogenesis Restores Dopaminergic Neuronal Loss in the Olfactory Bulb

Françoise Lazarini,[1,2] Marie-Madeleine Gabellec,[1,2] Carine Moigneu,[1,2] Fabrice de Chaumont,[3,4] Jean-Christophe Olivo-Marin,[3,4] and Pierre-Marie Lledo[1,2]

[1]Institut Pasteur, Laboratory for Perception and Memory, F-75015 Paris, France, [2]Centre National de la Recherche Scientifique, Unité Mixte de Recherche 3571, F-75015 Paris, France, [3]Institut Pasteur, Unité d'Analyse d'Images Quantitative, F-75015 Paris, France, and [4]Centre National de la Recherche Scientifique, Unité de Recherche Associée 2582, F-75015 Paris, France

Subventricular zone (SVZ) neurogenesis continuously provides new GABA- and dopamine (DA)-containing interneurons for the olfactory bulb (OB) in most adult mammals. DAergic interneurons are located in the glomerular layer (GL) where they participate in the processing of sensory inputs. To examine whether adult neurogenesis might contribute to regeneration after circuit injury in mice, we induce DAergic neuronal loss by injecting 6-hydroxydopamine (6-OHDA) in the dorsal GL or in the right substantia nigra pars compacta. We found that a 6-OHDA treatment of the OB produces olfactory deficits and local inflammation and partially decreases the number of neurons expressing the enzyme tyrosine hydroxylase (TH) near the injected site. Blockade of inflammation by minocycline treatment immediately after the 6-OHDA administration rescued neither TH^+ interneuron number nor the olfactory deficits, suggesting that the olfactory impairments are most likely linked to TH^+ cell death and not to microglial activation. TH^+ interneuron number was restored 1 month later. This rescue resulted at least in part from enhanced recruitment of immature neurons targeting the lesioned GL area. Seven days after 6-OHDA lesion in the OB, we found that the integration of lentivirus-labeled adult-born neurons was biased: newly formed neurons were preferentially incorporated into glomerular circuits of the lesioned area. Behavioral rehabilitation occurs 2 months after lesion. This study establishes a new model into which loss of DAergic cells could be compensated by recruiting newly formed neurons. We propose that adult neurogenesis not only replenishes the population of DAergic bulbar neurons but that it also restores olfactory sensory processing.

Key words: **adult neural stem cell; innate responses; interneuron; microglia; Parkinson's disease; regenerative medicine**

Introduction

In adult rodents, neural progenitor cells migrate from the subventricular zone (SVZ) of the forebrain through the rostral migratory system en route to the olfactory bulb (OB). These neuronal progenitors differentiate into at least three cell types once they reach the OB: granule cells (GCs), periglomerular neurons (PGNs), and short axon cells (SACs) (Carleton et al., 2003; Alvarez-Buylla and Lim, 2004; Lledo et al., 2006; Kosaka and Kosaka, 2008; Whitman and Greer, 2007; Adam and Mizrahi, 2010; Kiyokage et al., 2010). The vast majority of bulbar adult-born neurons turn into GCs that form inhibitory interneurons located in the deepest layer of the OB and that synapse on mitral cell secondary dendrites, on tufted cells, and possibly on other local interneurons (Mori et al., 1983; Lledo et al., 2008). In contrast, PGNs are located more superficially where they surround the glomeruli, whereas SACs are scattered throughout all OB layers. Both PGNs and SACs are chemically, morphologically, and functionally heterogeneous (Pignatelli et al., 2005, 2007, 2013; Parrish-Aungst et al., 2007; Kiyokage et al., 2010; Tan el al., 2010; Kosaka and Kosaka, 2012; Liu et al., 2013). In the OB circuit, tyrosine hydroxylase (TH), the rate-limiting enzyme required for the synthesis of dopamine (DA), is localized in neurons predominantly located in the glomerular layer (GL) that is composed of both PGNs and SACs. These two types of TH-expressing (TH^+) neurons also contain GABA and glutamic acid decarboxylase, the rate-limiting enzyme for GABA biosynthesis (Baker et al., 1983; Borisovska et al., 2013).

Although adult neurogenesis of GCs contributes to the neuronal replacement of old GCs throughout life, it ensures a continuous neuronal addition in the GL (Lagace et al., 2007; Ninkovic et al., 2007; Imayoshi et al., 2008; Adam and Mizrahi, 2011). These statements apply to the constitutive neurogenesis that takes place during adulthood, but it is not known whether adult neurogenesis could also replace neurons after acute DAer-

Received Dec. 23, 2013; revised Sept. 11, 2014; accepted Sept. 15, 2014.

Author contributions: F.L. and P.-M.L. designed research; F.L., M.-M.G., and C.M. performed research; F.d.C. and J.-C.O.-M. contributed unpublished reagents/analytic tools; F.L., M.-M.G., and C.M. analyzed data; F.L. and P.-M.L. wrote the paper.

This work was supported by Agence Nationale de la Recherche ANR-BLAN-SVSE4-LS-110624 and ANR-10-INBS-04-06 (FranceBioImaging), Laboratoire d'Excellence Revive Investissement d'Avenir ANR-10-LABX-73, and life insurance company Humanis group. We thank Ameyaltzin Castillo for initiating some of our behavioral experiments; Stéphanie Pons for advice on neurotoxin experiments; École des Neurosciences de Paris Ile-de-France vector platform for producing lentiviral vectors; and Matthew T. Valley, Gabriel Lepousez, and Gilles Gheusi for helpful comments on the manuscript.

The authors declare no competing financial interests.

Correspondence should be addressed to Dr. Pierre-Marie Lledo, Institut Pasteur, Perception and Memory laboratory, 25 rue du Dr. Roux, F-75724 Paris Cedex 15, France. E-mail: pmlledo@pasteur.fr.

DOI:10.1523/JNEUROSCI.5366-13.2014

 0270-6474/14/3414430-13$15.00/0

gic neuron depletion. Using chemical ablation of TH^+ cells, we investigate whether adult neurogenesis could restore the lesioned OB circuits and their associated olfactory-driven behaviors.

Materials and Methods

Mice, animal facilities, and ethic statements. In the course of this study, we used 2-month-old male C57BL/6J mice (Janvier Laboratories). Animals were housed in groups of four or five and maintained in standard conditions (controlled room temperature and humidity, 12 h/12 h light/dark cycle, with lights on at 8:00 A.M., *ad libitum* access to dry food pellets and water) at the Pasteur Institute animal care facilities, officially registered for experimental studies on rodents (Ministry approval number for animal care facilities, A 75-15-08; approval number 75-585 for animal experimentation). These studies were performed in compliance with the French legislation (Rural Code articles L 214-1 to L 214-122 and associated penal consequences), the European Communities Council Directive of 24 November 1986 (86/609/EEC), and European Union guidelines effective at the time the experimental studies were performed. All efforts were made to reduce mouse suffering and the number of animals used.

Chemical ablation of dopaminergic neurons. Stereotaxic injections were conducted as previously described (Pallotto et al., 2012). Mice were anesthetized intraperitoneally (120 mg/kg ketamine, Imalgene; 10 mg/kg xylazine Rompun, Bayer Health Care); 200 nl of 6-hydroxydopamine (6-OHDA), dissolved at 3 μg/μl in saline solution containing 0.03% ascorbic acid (Sigma), was stereotaxically injected (Nanoject II, Drummond) into the right substantia nigra (SN) pars compacta or in each OB using the following coordinates from the pial surface: OB, anteroposterior (AP) 5 mm, mediolateral (ML) ±0.75 mm, dorsoventral (DV) 0.3; SN, AP −3 mm, ML 1.2 mm, DV 4.3 mm (see Fig. 1*A*). Vehicle controls were injected with only saline solution containing 0.03% ascorbic acid.

Labeling of new neurons. To label proliferating cells, mice were injected intraperitoneally with a DNA synthesis marker, BrdU (Sigma), at 100 mg/kg in 0.9% NaCl, 2 h before perfusion. To study the distribution of new neurons, we used lentiviral vectors as previously described (Pallotto et al., 2012); 200 nl of a replication-deficient lentivirus expressing eGFP under control of the CMV promoter (custom-built LV-CMV-GFP with a viral titer of 10^9 units/ml) (Mejia-Gervacio et al., 2012) was stereotaxically injected into each rostral migratory stream (RMS) (AP 3.3 mm, ML ±0.82 mm, DV −2.90 mm from the pial surface) to label SVZ-generated neuroblasts that migrate toward the OB.

Anti-inflammatory treatment. Minocycline (Sigma-Aldrich), freshly dissolved in sterilized 0.9% NaCl (saline), or saline alone was injected intraperitoneally during 7 weeks. On day 1, 6-OHDA, or its vehicle, was injected into the two dorsal OBs, as described above. Mice were treated with minocycline (50 mg/kg) twice daily for the first 2 d (8 h interval) and once daily for the next 5 d as previously described (Lazarini et al., 2012).

Rotarod test. This test assesses the ability of an animal to maintain balance on a rotating 4.5-cm-diameter rod (Bioseb) that depends both on motor ability and coordination. Unilateral lesions of motor brain areas affect the balance. Mice were subjected to three trials separated by 10 min intervals and during which the rotation speed accelerates from 4 to 40 rpm in 5 min. The latency to falling is used to assess the balance performance, and the mean latency is calculated for each mouse.

Innate olfactory test. We used an olfactory test that depends on innate behavioral responses as previously described (Lazarini et al., 2012). All experiments were performed under light illumination (100 Lux) during the light period (1:00 to 6:00 P.M.) in dedicated rooms. A video camera fixed to the ceiling was connected to a computer situated outside the test room, and the behavior was analyzed using a video-track system (Viewpoint). The test cages were made of open boxes (36 × 24 × 29 cm) with two compartments separated by an aluminum separator (holes 0.5 cm diameter). The lower compartment was 2.5 cm high. For the Coco Pops test, mice were fasted for 20 h before testing. A session of the innate olfactory test is divided into four stages: acclimation, habituation, biexposure to vehicle, and exposure to the tested smell and its vehicle. Mice were acclimated individually in a cage similar to the test cage for 20 min before testing. Mice were first habituated to the test cage during 10 min and then exposed to 40 μl of smell solution by placing a filter paper dish (70 mm) in the lower compartment in both zone 1 (vehicle or smell) and zone 3 (vehicle only). Mice were subjected to two successive trials, separated by a 5 min interval: the first trial is vehicle trial, with 3 min exposition to the vehicle in both zones 1 and 3; the second trial is smell trial, with 3 min exposure to the tested smell in zone 1 and exposure to its corresponding vehicle in zone 3. The tested smells and their respective vehicles are the following:

Aversive smells. As a nonsocial aversive odor, we used 2-methylbutyric acid (2-MB acid, Sigma) dissolved at 10^{-4} M in water. For a predator odor cue, we used a constituent of fox anal secretion known to trigger innate fear responses in rodents: 2,4,5-trimethylthiazoline (TMT, Con-Tech) diluted in 2% mineral oil (MO).

Attractive smells. As a nonsocial attractive smell, we used Coco Pops cereals (Kellogg's; 5 pellets, fixed with patafix on Parafilm) with corresponding control cues made of patafix on Parafilm. For a social smell cue, we pooled pure female urine, and we used water as control. Urines were collected from five adult C57BL/6 females by gently massaging the pelvic region. The urine was collected with a glass Pasteur pipette as soon as it was spontaneously voided above a glass Petri dish. Urine samples were subsequently pooled and stored at −20°C until the test.

Neutral smells: water, undiluted MO, or "Parafilm." Mice were subjected to only one presentation of each tested smell, during only one session of two trials per day. Using the video-track system, both trajectory and time spent in each zone were determined at day 11 and day 28 after lesion. We calculated the preference index as the difference between the times spent during the trial 2 in the scented zone 1 with a smell (neutral, aversive, or attractive) as a stimulus, and with its vehicle (water, MO, or "Parafilm") as a stimulus.

Immunohistochemistry. Forty-micron-thick coronal or sagittal sections were made using a vibrating microtome (VT1000S, Leica), except for experiments with viral labeling of neuroblasts in which 60-μm-thick coronal sections were vibro-sliced. All immunostaining was performed on free-floating sections. Slices were blocked in 0.2% Triton, 4% BSA (Sigma), and 2% goat serum and incubated overnight with primary antibodies at 4°C followed by an incubation step with secondary antibodies (biotinylated or Alexa-conjugated secondary antibodies, Jackson ImmunoResearch Laboratories) at room temperature. Primary antibodies used in this study and their working dilutions are listed in Table 1. For immunolabeling of TH, GFAP, doublecortin (DCX), and cluster of differentiation (CD) 68, brain sections were preincubated for 20 min in citrate buffer 0.1 M, pH 9.0, at 80°C. For BrdU staining, DNA was denatured with 2 N HCl for 30 min at 37°C. Fluorescent sections were stained with the nuclear dye DAPI and then mounted in a solution of 1,4-diazabicyclo[2.2.2]octano (Sigma). Immunoperoxidase-labeled cells were developed using the ABC system (Vector Laboratories) and 3,3′-diaminobenzidine (0.05%, Sigma) as chromogen, and then sections were mounted in Depex medium.

Image acquisition and quantification analysis. For each animal, six to eight coronal sections 40 μm apart were selected, using the accessory OB as a landmark. For sagittal sections, six consecutive slices containing both SVZ and RMS were selected. Reconstructed images of the OB or SVZ and RMS were taken using an Apotome microscope (Aviovert 200M; Zeiss) with a 25× objective or an Olympus BX51 microscope with a 20× objective and Compix Imaging software (Hamamatsu Photonics). Double immunofluorescence staining was analyzed in three dimensions using a confocal laser-scanning microscope (LSM 710; Zeiss) with Zen Imaging software (Zeiss) as previously described (Lazarini et al., 2012). Photoshop CC software (Adobe Systems) was used to delineate the area of interest: images of the OB coronal sections were divided into eight sectors of equal 45° angle, starting from the middle of the dorsal portion of the GL and ending clockwise to the point (see Fig. 1*B*). The "injected area" is defined as the dorsal domain of the OB (coronal section) located from −45° to 45° (see Fig. 1*B*) and the "nonlesioned area" comprises the rest of the OB section. For TH, BrdU, and active caspase (casp) 3 staining in the OB, labeled cells were manually counted (6 slices per animal; 3 or 4 animals were analyzed per group) in the injected and nonlesioned area of both the GL and the granular cell layer (GCL) using Photoshop images. For double (GFP/TH) staining, all GFP^+ cells present in the GL were first individually localized in the GL (both noninjected and injected areas) by

Table 1. Detailed information on the primary antibodies used in this study

Antibody (anti)	Manufacturer and catalog no.	Marker of:	Working dilution
BrdU	Abcys, ABC 117-7513	Proliferating cells	1:1000
	Megabase Research Products		1:2000
Calb	Swant, 300	Calbindin-interneurons	1:2000
active casp3	Cell Signaling, asp175	Apoptotic cells	1:300
CD68	Serotec, MCA1957GA	Activated microglia	0.5 μg/ml
DCX	Abcam, ab 18723	Neuroblasts	0.5 μg/ml
GFAP	Dako, 20334	Astrocytes	4 μg/ml
Iba1	Wako Chemicals, 016-20001	Microglia	1 μg/ml
NeuN	Millipore Bioscience Research Reagents, MAB377	Neurons	5 μg/ml
Olig2	Santa Cruz Biotechnology, sc48817	Oligodendrocyte progenitors	1:500
Pax6	Millipore Bioscience Research Reagents, AB2237	Dopaminergic neurons	1:700
TH	ImmunoStar, 22941	Dopaminergic neurons	1:4000

using Photoshop on reconstructed apotome images before further classification in TH^+- or TH^--expressing cells using confocal microscopy (LSM 710 Zeiss). For Calbindin (Calb), Pax6, Olig2, and DCX staining in the OB, as well as BrdU staining in the SVZ and RMS, quantification has been performed using the open source platform Icy (de Chaumont et al., 2012) (http://www.icy.bioimageanalysis.org). The detection of labeled cells has been performed using a multiscale approach based on wavelets (Olivo-Marin, 2002) implemented in the plugin Spot detector (http://icy.bioimageanalysis.org/plugin/Spot_Detector). Regions of interest ("injected" area, no-lesioned area; see Fig. 1*B*) have been designed interactively with a protractor widget and the plugin Protractor ROI Cutter (http://icy.bioimageanalysis.org/plugin/Protractor_ROI_Cutter) in association with the ring plugin (http://icy.bioimageanalysis.org/plugin/RingROI). Pax6-positive cell number was assessed in the superficial area (40% of the external-internal axis) of the dorsal GCL located from −45° to 45°. For the quantification of DCX immunoreactivity, the pixel density is computed using the plugin Thresholded pixel density. This plugin computes the number of pixels over a threshold in a given region of interest over the total number of pixels present in the region of interest (http://icy.bioimageanalysis.org/plugin/Thresholded_pixel_density). The batch mode of this analysis is available as a protocol: http://icy.bioimageanalysis.org/protocol/Pixel_density_(batch_mode). All the code and implementation of those programs are available online. Data are expressed as optical density of staining (pixels per mm^2), number of simple-labeled cells or double-labeled cells, percentage of double-labeled cells present in the injected or nonlesioned area (GL, GCL) or ratio of simple-labeled cells or double-labeled cells in the injected area over that in the nonlesioned area.

Statistical analyses. All data are expressed as mean ± SEM. Statistical analyses were performed using Prism software (GraphPad, version 6), with $p < 0.05$ considered significant. Data were analyzed using parametric tests: unpaired or paired two-tailed Student's *t* test, one-way ANOVA or two-way ANOVA followed by Bonferroni *post hoc* test, when appropriate.

Results

Transient ablation of DAergic interneurons in the OB

DAergic interneurons in the OB are located in the GL where they participate in olfactory processing by acting in concert on the following: (1) sensory afferent nerve terminals, (2) projection neurons (i.e., mitral/tufted cells), and (3) local PGNs (Murphy et al., 2005). These interneurons belong to a subset of PGNs that are continuously generated throughout life (Halász et al., 1977; Parrish-Aungst et al., 2007). 6-OHDA, a hydroxylated analog of dopamine, selectively eliminates OB DAergic interneurons in a manner similar to its action in the ventral tegmental area and the SN (Sotelo et al., 1973; Willis et al., 1976). We evaluated the impact of lesioning the bulbar DAergic interneurons by stereotaxic injection of 6-OHDA into the OB (Fig. 1*A*), or into the right SN pars compacta as a control (Fig. 1*A*). 6-OHDA was applied using the same dose as used previously in Parkinson's disease (PD) models (Sotelo et al., 1973; Höglinger et al., 2004). Immunohistochemical analysis revealed that injection of 6-OHDA in the dorsal OB led to a selective reduction in TH^+ cells restricted to the dorsal portion of the GL (Fig. 1*B*). In contrast, injections into the right SN pars compacta dramatically reduced TH labeling in the right striatum and in the right SVZ, revealing the strong DAergic denervation of these two areas ($n = 4$; Fig. 1*C*, left), whereas the contralateral striatum and SVZ were unchanged, demonstrating the specificity of the injury ($n = 4$; Fig. 1*C*, left). We found no change in the striatal and SVZ immunoreactivity for TH when 6-OHDA was locally injected in the OB (Fig. 1*C*, right), indicating absence of retrograde diffusion from the OB to the forebrain and confirming the absence of long-range projections from bulbar DA-containing neurons.

After the 6-OHDA injection in the OB, we found a partial (40%) and transient decrease in the number of TH-expressing neurons located in the lesioned dorsal part of the OB at 7 d after injection (Fig. 1*D*,*G*; day 7 after lesion, $t_{(6)} = 2.877$, $p = 0.0282$). We investigated whether 6-OHDA induces cell apoptosis by assessing activated caspase 3-positive dying cells in the injected area at 6 h, 1 d, 3 d, and 7 d after lesion. We found a significant increase in activated caspase 3 at day 3 after 6-OHDA injection (Fig. 1*F*), which was subsided at day 7, suggesting that the loss of TH^+ probably resulted from DAergic cells loss rather than a change in cell phenotype. This DAergic ablation occurred only in the 6-OHDA-injected area but not in the nonlesioned area, defining the extent and specificity of the 6-OHDA lesion (the number of TH^+ cells in the nonlesioned area at day 7 after lesion was 14,342 ± 2594 with vehicle and 14,776 ± 1631 with 6-OHDA; $t_{(6)} = 0.1417$, $p = 0.892$). Similar effects were seen at 14 d after injection, but already at 21 d after injection, the number of TH^+ cells in the injected area recovered to ~80% of the vehicle; and at 56 d after injection, no statistical difference could be seen between vehicle- and treated-mice ($n = 4$ or 5 per group; Fig. 1*G*).

Because a subpopulation of superficial GC derived from Pax6-expressing progenitors also expresses mRNA for TH (Kohwi et al., 2005), we have investigated whether 6-OHDA injections might target also those deep neurons. We delineated the area of interest (superficial 40% part of the dorsal GCL, located in the "injected area" defined as in Fig. 1*B*) and then assessed the number of Pax6-positive cells in this GCL zone. We found no difference at day 7 after lesion between vehicle and 6-OHDA-injected mice (vehicle: 4261 ± 343 Pax6-positive cells, 6-OHDA: 4341 ± 347 Pax6-positive cells), indicating that 6-OHDA injections into the dorsal GL did not eliminate Pax6-expressing GCs. Conversely, we found no change at day 7 after lesion in the lesioned region for the number of another PG population subtype, the

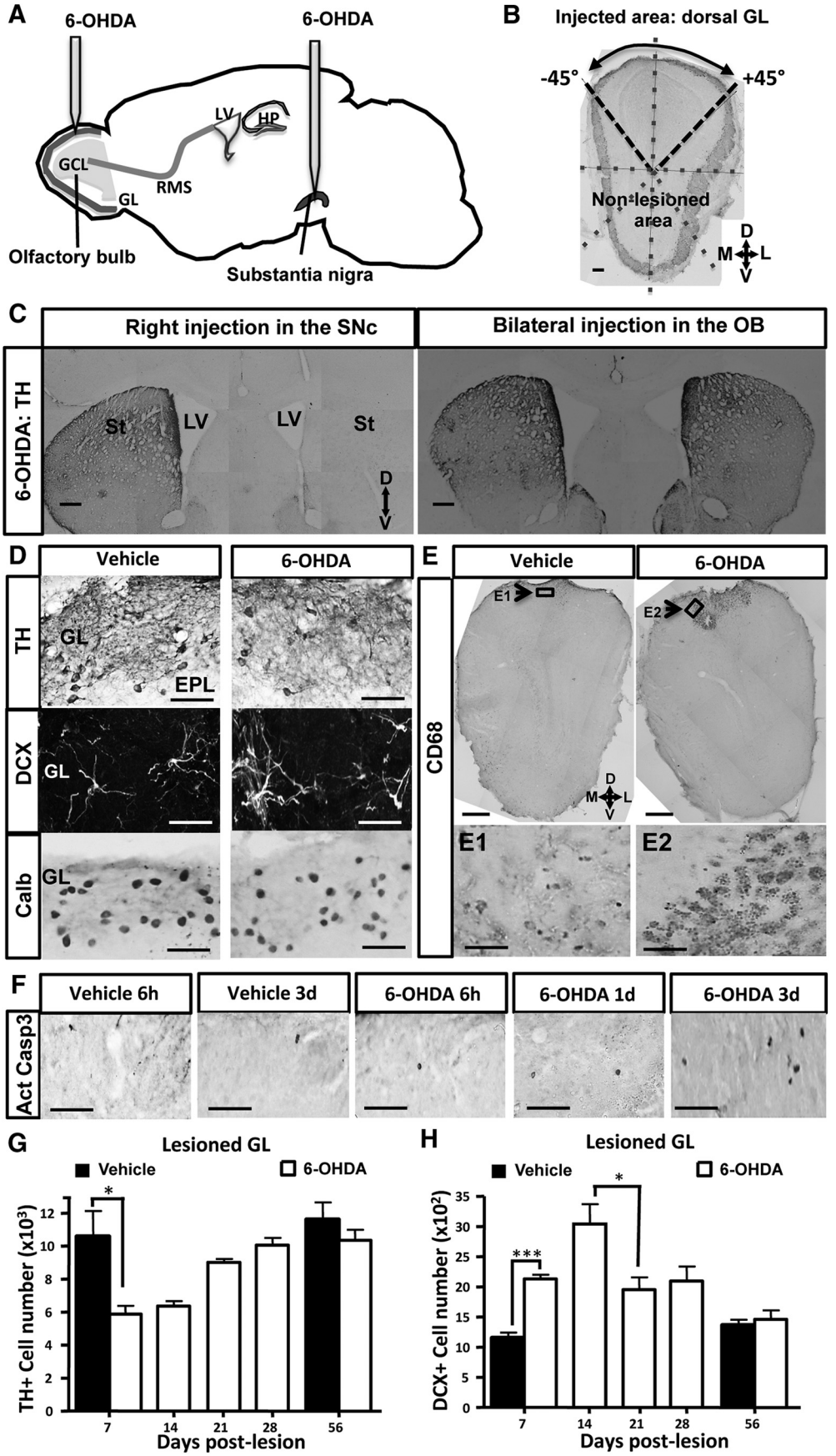

Figure 1. Transient dopamine cell loss after a 6-OHDA-induced lesion of the OB. ***A***, Design of the experimental procedure. A 6-OHDA-containing solution, or vehicle alone, was infused into the right SN or into the dorsal part of each OB. ***B***, TH immunostaining delineates the injected and noninjected areas in a coronal OB section. The image was divided (*Figure legend continues.*)

Calb-positive interneurons (Fig. 1*D*, bottom panels; the number of Calb-positive cells in the lesioned dorsal part of GL at day 7 after lesion was 10,341 ± 847 with vehicle and 8373 ± 1289 with 6-OHDA; $t_{(4)} = 1.277$ and $p = 0.271$). These data indicate that 6-OHDA did not unspecifically alter the dorsal GL, but only DAergic cells. In line with this, we found no statistical difference at day 7 after lesion for the thickness of the dorsal GL measured in vehicle and 6-OHDA-treated mice (from coronal OB sections, the areas of dorsal GL located from −45° to 45° were in vehicle: $1.15 \pm 0.08 \times 10^{-2}$ mm^2; and in 6-OHDA: $1.32 \pm 0.16 \times 10^{-2}$ mm^2; $t_{(4)} = 0.943$, $p = 0.3991$). We conclude that a local 6-OHDA injection results in a spatially restricted transient loss of DAergic PGNs in the dorsal portion of the OB.

Activation of microglia in the lesioned portion of the OB

6-OHDA is suspected not only to directly trigger cell death of DAergic neurons by oxidative stress induction and mitochondrial inhibition, but studies in other brain areas have also reported indirect DAergic cell elimination by activated microglia (Akiyama and McGeer, 1989; Du et al., 2001; He et al., 2001; Wu et al., 2002; Virgone-Carlotta et al., 2013). To check whether the DAergic PGN lesion could activate microglia cells, we performed CD68 staining (Fig. 1*E*) to quantify the number of activated microglia. We have already shown in the OB that CD68 is strongly expressed by activated microglial cells after acute sensory deafferentation (Lazarini et al., 2012). Here, we found strong staining for CD68 in the 6-OHDA-injected OB at 7 d after lesion, with a fivefold increase in 6-OHDA-injected animals compared with vehicle-treated mice. Activated microglia were present only in the dorsal part of the OB corresponding to the injected area (Fig. 1*E*), and this activation was found to be transient since we observed only faint staining for CD68 at 1 month after lesion (data not shown). The dorsal neuroinflammation was not restricted to the GL, but it extended deeper to the external plexiform layer and the GCL, delineating a cone with a base located at the surface of the dorsal GL and the tip oriented toward the GCL. The activation of microglia was specific to the 6-OHDA-treated OB but not due to invasive surgery as shown by faint staining for CD68 in vehicle-treated mice (Fig. 1*E*).

The number of DCX-positive neurons increases in the lesioned OB

To assess whether the local DAergic cell loss could influence the processes of adult neurogenesis, we quantified the number of adult-born neurons located in the injected area during the first 2 months after lesion (i.e., at 7, 14, 21, 28, and 56 d after lesion). We counted the number of developing adult-born neurons by quantifying the numbers of DCX, a neuronal marker transiently expressed by newly generated neurons (Brown et al., 2003) (Fig. 1*D*,*H*). We observed a strong increase in DCX-positive cells in the GL of injected area of lesioned mice peaking at 14 d after 6-OHDA lesion and recovering 7 d later (Fig. 1*H*; day 7 after lesion, $t_{(5)} = 8.151$; $p = 0.0005$). Conversely, we found no change in the number of DCX-positive cells in the GL of nonlesioned area of the same mice (day 7 after lesion, vehicle: 102.3 ± 0.9 DCX-positive cells; 6-OHDA: 99.3 ± 4.3 DCX-positive cells; $t_{(4)} = 0.695$, $p = 0.528$). Moreover, we found no change in DCX immunoreactivity in both RMS of the OB (RMSob) and GCL of injected area or nonlesioned area (Fig. 2*C*). Thus, 6-OHDA lesioning has only local effects on the DCX cell number by increasing this number in the lesioned GL area but sparing the other OB regions.

To check whether the increased number of DCX-positive immature neurons found in the lesioned GL could result from local proliferation or change in SVZ proliferation, the cell proliferation marker BrdU was injected 2 h before perfusion at 7 d after lesion (Fig. 2*A*). This protocol allows labeling of proliferating cells, including dividing precursor cells along the SVZ-RMS (Fig. 2*B*). No difference in BrdU-positive cell density within the SVZ and the RMS was found between vehicle and 6-OHDA-treated groups (Fig. 2*B3*; treatment effect, $F_{(1,12)} = 0.0596$, $p = 0.8112$). This result indicates that 6-OHDA OB lesioning did not alter proliferation or migration of adult-generated interneurons. However, we observed a strong increase in proliferating BrdU-positive cells in the dorsal part of the 6-OHDA-lesioned OB (Fig. 3*A*,*B*; $t_{(6)} = 5.113$, $p = 0.0022$) where the BrdU immunoreactivity was restricted to a cone-shaped area located in the most superficial zone pointing toward the GCL. Figure 3*A* shows the extent and specificity of the lesioned areas. To identify which cell population was proliferating, we analyzed the phenotype of BrdU-positive cells (Fig. 3*C*,*D*). A total of 97% of BrdU-positive cells were colabeled by the microglial-specific antibody IBA1 (Fig. 3*C1*), revealing their microglia nature. In contrast, no BrdU-positive cells were costained with immature neuron (DCX)-specific antibody, indicating absence of neuronal proliferation in the region of DAergic cell loss.

Finally, to address whether the increased number of DCX-positive cells found in the lesioned GL could result from local proliferation of oligodendrocyte progenitors as previously shown (Jablonska et al., 2010), the number of cells positive for the transcription factor Olig2, a marker of oligodendrogenesis and of neuronal precursors (Zhou and Anderson, 2002), was assessed at 7 d after lesion. We found no change in the number of Olig2-positive cells in the GL of lesioned area (dorsal area located between −45° and 45°) of the same mice (day 7 after lesion, vehicle: 4261 ± 343 Olig2-positive cells; 6-OHDA: 4341 ± 347 Olig2-positive cells; $t_{(4)} = 0.165$, $p = 0.877$). Thus, 6-OHDA lesioning of the dorsal GL results in a strong neuroinflammation that is restricted to the dorsal part of the OB but extends to all OB layers and leads to local microglial activation and proliferation, but not to neuronal precursor or oligodendrocyte progenitor proliferation.

←

(*Figure legend continued.*) into 8 sectors of 45°. ***C***, TH immunoreactivity of coronal sections of striata and SVZ at 1 month after 6-OHDA injection into the right SN (left) or the two OBs (right). The efficacy of DA denervation is demonstrated by low levels of TH expression in the right striatum and right SVZ after neurotoxin injection into the right SN (left), depicting the extent and specificity of the lesion. Conversely, the right panel represents no alteration of TH expression in the two striata and SVZ after injection of 6-OHDA into the OB. ***D***, Immunoreactivity for TH (top), DCX (middle), and Calb (bottom) of the lesioned GL at 7 d after injection into the OB of vehicle (left) or 6-OHDA (right). 6-OHDA reduces the number of DAergic cells expressing TH in the dorsal GL. Conversely, 6-OHDA increases DCX number but does not change Calb number in the same area. ***E***, Immunoreactivity for CD68 (***E1***, ***E2***, top) of the dorsal OB at 7 d after injection into the OB of vehicle (left) or 6-OHDA (right). 6-OHDA activates microglial cells as revealed by CD68 staining. Note the restricted presence of activated microglia in the dorsal part of the OB, depicting the extent and specificity of the lesion. Arrow indicates the area shown at higher magnification in ***E1*** and ***E2***. ***F***, Time course of apoptotic cells expressing active cleaved casp 3 in the lesioned GL after 6 h, 1 d, and 3 d after 6-OHDA injection. The number of apoptotic cells is increased at day 3 after OB lesion. ***G***, Time course of TH$^+$ PGNs located in the lesioned GL after OB lesion ($n = 4$ or 5 animals per group). The number of TH-expressing neurons is transiently reduced in the dorsal GL after OB lesion. ***H***, Time course of DCX-positive PGNs located in the lesioned GL after OB lesion ($n = 4$ or 5 per group). The number of developing neurons expressing DCX peaks at day 14 in the dorsal GL after OB lesion and resumes 21 d later. $^*p < 0.05$. $^{***}p < 0.001$. Scale bars: ***B***, ***C***, 100 μm; ***D***, 20 μm; ***E***, 100 μm; ***E1***, ***E2***, 20 μm.

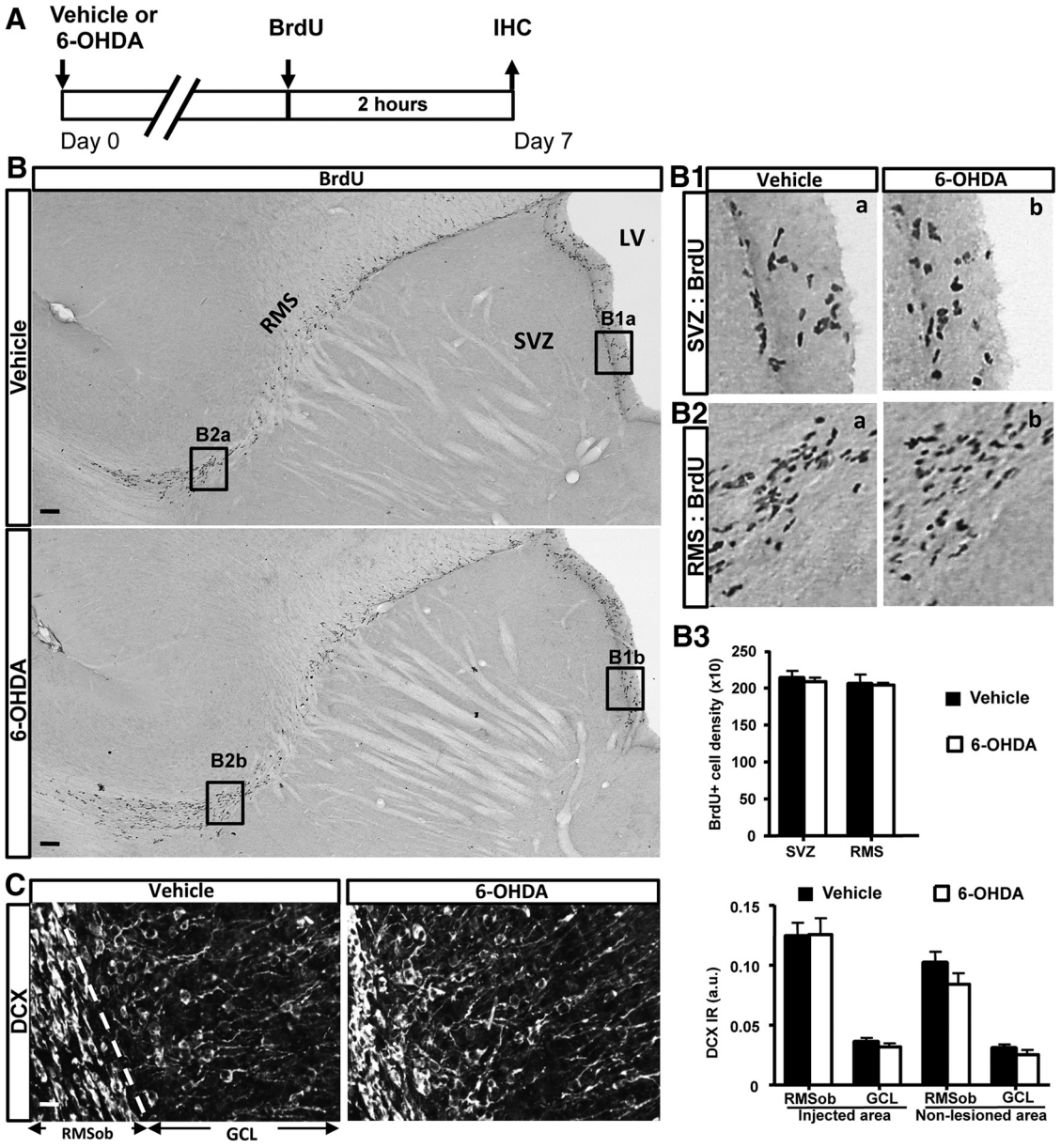

Figure 2. 6-OHDA-induced lesion of the OB spares the first steps of neurogenesis. ***A***, Design of the experiments. Vehicle, or 6-OHDA, was bilaterally injected into the GL, and mice were perfused 7 d later. To label proliferating cells, BrdU was injected 2 h before perfusion. ***B***, Sagittal sections of the forebrain injected with vehicle (top) or 6-OHDA (bottom) showing the different neurogenic zones labeled with BrdU. ***B1***, ***B2***, Higher magnifications of areas indicated in the sections. ***B3***, BrdU-positive cell density in the SVZ and RMS at day 7 after lesioning. ***C***, Coronal sections of the OB of vehicle (left) or 6-OHDA (middle) showing the RMSob and the GCL labeled with DCX. Right, DCX immunoreactivity (IR, in arbitrary units, a.u.) in the RMSob and GCL of injected and nonlesioned areas quantified 7 d after lesion. Scale bars: ***B***, 250 μm; ***C***, 25 μm.

DAergic cell loss facilitates incorporation of adult-born PGNs

The increased number of developing neurons in the injection area during the first 2 weeks after 6-OHDA treatment could result from increased recruitment of newly generated neurons that migrate tangentially in the RMS, from increased numbers of radially migrating young neurons in the OB, or from both enhanced migratory processes. To tackle this question, a replication-defective lentivirus expressing GFP was bilaterally injected to the RMS of mice to label migrating newborn cells at the time of injection (Fig. 4*A*,*B*). Seven days later, vehicle or 6-OHDA was bilaterally injected into the GL. First, we assessed the number of PGNs expressing both TH and GFP in the injected area at day 14 after the viral vector injection. In vehicle mice, only 10 ± 1% of GFP-positive cells also express TH (from 136 counted GFP-positive cells analyzed among 4 mice). In 6-OHDA-injected OB, only 10 ± 2% of GFP-positive cells also express TH (from 134 GFP-positive cells analyzed among 4 mice). We found no difference between the two groups of mice ($t_{(4)} = 0.644$, $p = 0.554$), suggesting that 6-OHDA lesion does not change the proportion of new DAergic PGNs integrating the OB network. However, 6-OHDA could change the survival of PGNs, increasing their number in the lesioned OB network. To address this issue, because labeling efficiency varied among mice (data not shown), we analyzed the relative number of GFP-labeled new neurons found in the injected area compared with those located in the nonlesioned area 14 d after viral injection (Fig. 4*C*). This ratio evaluates whether PGNs and GCs are specifically recruited into 6-OHDA-treated or vehicle-treated OB areas. Although no difference was

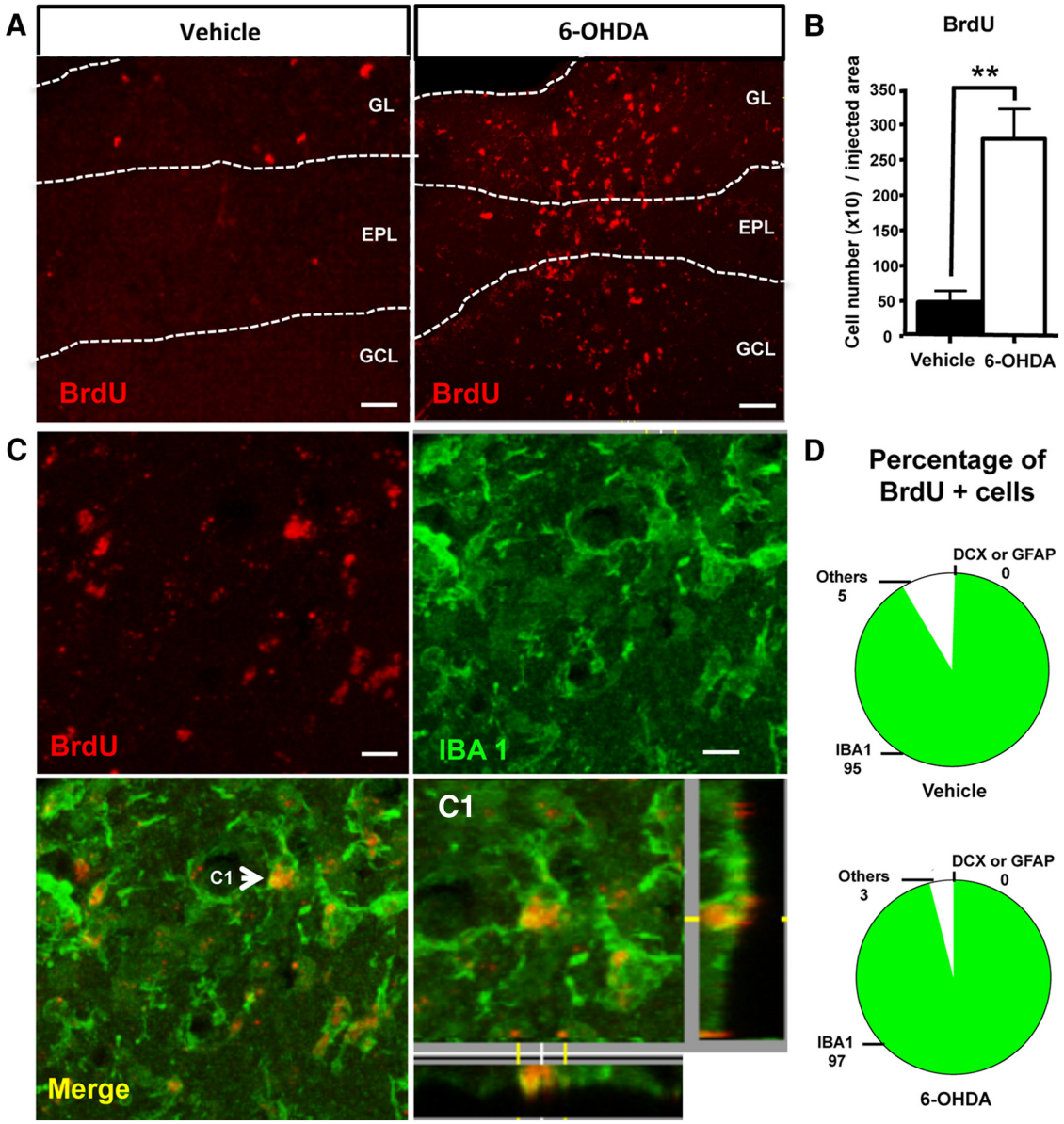

Figure 3. Microglial cells, but not neuroblasts, proliferate in the 6-OHDA-lesioned OB. ***A***, BrdU immunostaining in the OB of a vehicle (left) and a 6-OHDA-injected OB (right) at 7 d after lesion. BrdU-positive cells were restricted to the dorsal part of the OB, mainly in the GL, but also in the external plexiform layer and GCL. ***B***, Quantification of BrdU-positive cells in the injected area (dorsal part of the OB) at 7 d after lesion ($n = 4$ mice per group). ***C***, BrdU and IBA1 immunostaining in the GL of a 6-OHDA-injected OB at 7 d after lesion. BrdU was only found in microglial cells expressing IBA1. Arrow indicates the cell shown at higher magnification in ***C1***. ***D***, Percentage of BrdU-positive cells colabeled with one of three cell markers: GFAP for astrocytes, DCX for developing neurons, and IBA1 for active microglial cells. Cell counts were performed in the dorsal GL of vehicle and 6-OHDA-lesioned mice at 7 d after lesion ($n = 4$ mice per group, ~100 cells analyzed per mouse). Nearly all fast-proliferating cells positive for BrdU coexpressed IBA1. $^{**}p < 0.01$, compared with vehicle. Scale bars: ***A***, 50 μm; ***C***, 10 μm.

found between 6-OHDA and vehicle-treated mice regarding adult-born GCs, this ratio significantly increased for PGNs (Fig. 4*C*; $t_{(6)} = 3.006$, $p = 0.0238$). This observation indicates that migration/integration of immature PGNs was biased toward the 6-OHDA-injected area. Thus, PGNs preferentially integrated into the area in which DAergic PGNs were selectively lost and where microglia were activated. We conclude that 6-OHDA administration into the dorsal OB results in a regional DAergic cell loss followed by a complete recovery of TH^+ PGNs, at 4 weeks after lesion, and this recovery might result, at least in part, from increased incorporation of adult-born PGNs in the ablated area.

Behavioral consequences of the DAergic cells loss and recovery

Given the dramatic effects of 6-OHDA on bulbar DAergic interneurons, we investigated possible consequences on olfactory-driven behaviors. First, because of potential concerns using 6-OHDA on locomotion, we checked the motor activity of treated mice using a Rotarod (Fig. 5*A*). Mice were tested at 1 and 4 weeks after intrabulbar injection. Whereas mice subjected to 6-OHDA infusion into the right SN showed lower balance performance than controls, we found no motor deficits in mice injected with 6-OHDA compared with vehicle mice (Fig. 5*A*; $F_{(5,79)} = 3.04$, $p = 0.0146$; mice injected in the right SN, 6-OHDA

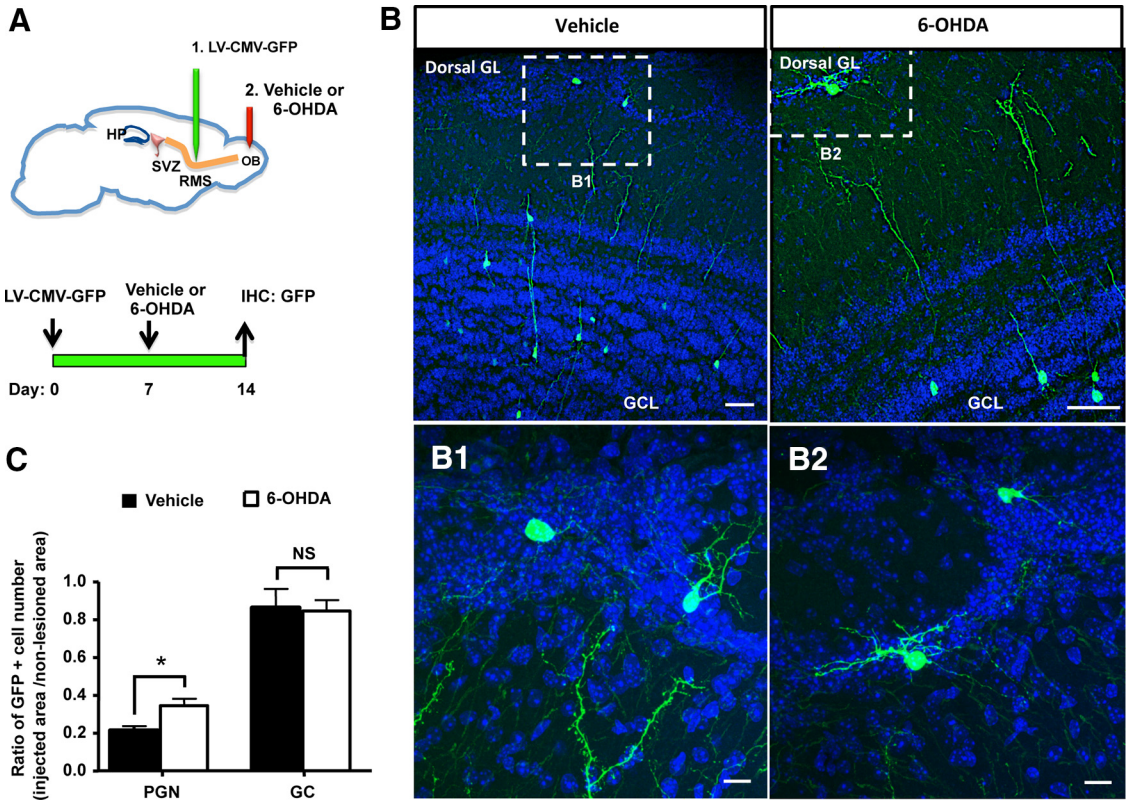

Figure 4. Preferential incorporation of lentivirus-labeled adult-born PGNs in the local area of DAergic neuron ablation. ***A***, Overview of the experimental procedure. Mice were bilaterally injected into the RMS by a replication-defective lentivirus expressing eGFP to label migrating newborn cells at the time of injection. Seven days later, vehicle, or 6-OHDA, was bilaterally injected into the GL, and mice were analyzed 2 weeks later. ***B***, GFP staining in the dorsal OB at 2 weeks after viral injection in vehicle and 6-OHDA-lesioned mice. ***B1***, ***B2***, Delineated areas are shown at higher magnification. ***C***, Ratio of the number of virus-labeled new neurons in the injected area over the one counted in the noninjected area ($n = 4$ mice per group). This ratio is more elevated for PGN in 6-OHDA-injected mice, indicating a bias for incorporating immature neurons into the lesioned area. *$p < 0.05$, compared with vehicle. NS, Not significant. Scale bars: ***B1***, ***B2***, 20 μm.

compared with vehicle: $t_{(21)} = 4.167$, $p = 0.0004$). These data indicate that a local 6-OHDA lesion in the OB had no functional impact on motor coordination.

Next, we assessed distinct olfactory-driven behaviors after 6-OHDA treatments 7 d after lesion. Innate olfactory tests were performed using aversive, attractive, and neutral olfactory cues, as previously described (Lazarini et al., 2012). Aversive odorants consisted of 2-MB acid, a nonsocial odorant cue emitted by spoiled foods, and TMT, a predator odorant found in fox urine (Kobayakawa et al., 2007). The attractive olfactory cue consisted of Coco Pops cereal, a source of food smells, and pool of conspecific female urines as a social smell cue (Nyby et al., 1985; Feierstein et al., 2010; Malkesman et al., 2010; Lazarini et al., 2012). As for controls, we used neutral sources of odorants, such as water, MO, and plastic paraffin film (hereafter called Parafilm). We assessed a preference index for each olfactory cue by calculating the difference between the time spent in the scented zone during the odorant trial minus the time spent in the scented zone during vehicle presentation. As expected, all mice exhibited similar olfactory behavior when using neutral olfactory cues (Fig. 5*B*). In contrast, Coco Pops cereals were attractive for both vehicle and 6-OHDA-lesioned mice because they were found to spend more time in the scented zone (Fig. 5*B*; vehicle mice: Coco-Pops vs Parafilm, $t_{(29)} = 4.083$, $p = 0.0003$; 6-OHDA mice: Coco-Pops vs Parafilm, $t_{(28)} = 1.712$, $p = 0.049$). As a result, the preference index for Coco Pops was strongly positive for both vehicle- and 6-OHDA-treated mice (Fig. 5*C*), indicating unchanged attraction for food smells after 6-OHDA lesion.

In sharp contrast with these results, when we used attractive female urine or aversive olfactory cues, mice were strongly impaired after OB lesions with 6-OHDA (Fig. 5*B*,*C*). Consistent with previous reports (Kobayakawa et al., 2007; Dewan et al., 2013), vehicle-treated mice showed standard avoidance responses to either 2-MB acid or TMT, spending more time in the cage zones far away from the odorant source (Fig. 5*B*; top 2 and 3, 2-MB acid vs water: $t_{(35)} = 4.237$, $p = 0.0002$; TMT vs MO: $t_{(30)} = 3.109$, $p = 0.0041$). Thus, olfactory behaviors of 6-OHDA-treated mice substantially differ from control mice (Fig. 5*B*,*C*; 2-MB acid: vehicle vs 6-OHDA mice, $t_{(34)} = 4.271$, $p < 0.0001$; TMT: vehicle vs 6-OHDA mice: $t_{(30)} = 3.240$, $p = 0.0029$). Surprisingly, 6-OHDA-treated mice exhibited a noninterest, or even attraction, to the aversive odorants (Fig. 5*B*, bottom 2 and 3). On the other hand, vehicle mice showed attractive response to female urine, spending more time in the scented zone (Fig. 5*B*, top 4, female urine vs water: $t_{(33)} = 3.473$, $p < 0.0015$), whereas 6-OHDA-lesioned mice showed no interest, or repulsion, to female urine (Fig. 5*B*, bottom 4; vehicle vs 6-OHDA mice: $t_{(33)} = 4.433$, $p < 0.0001$).

Collectively, these data indicate that a 6-OHDA lesion of the OB impairs innate behavioral responses triggered by nonsocial and social olfactory cues. Finally, we evaluated the impact of DAergic cell loss and recovery on TMT olfactory responses observed at different time points: 7 d, 1 month, and 2 months after 6-OHDA treatment (Fig. 5*D*). We found a significant difference in TMT responses between the vehicle and 6-OHDA groups at both 1 week and 1 month after injection (Fig. 5*D*; $F_{(5,91)} = 3.441$,

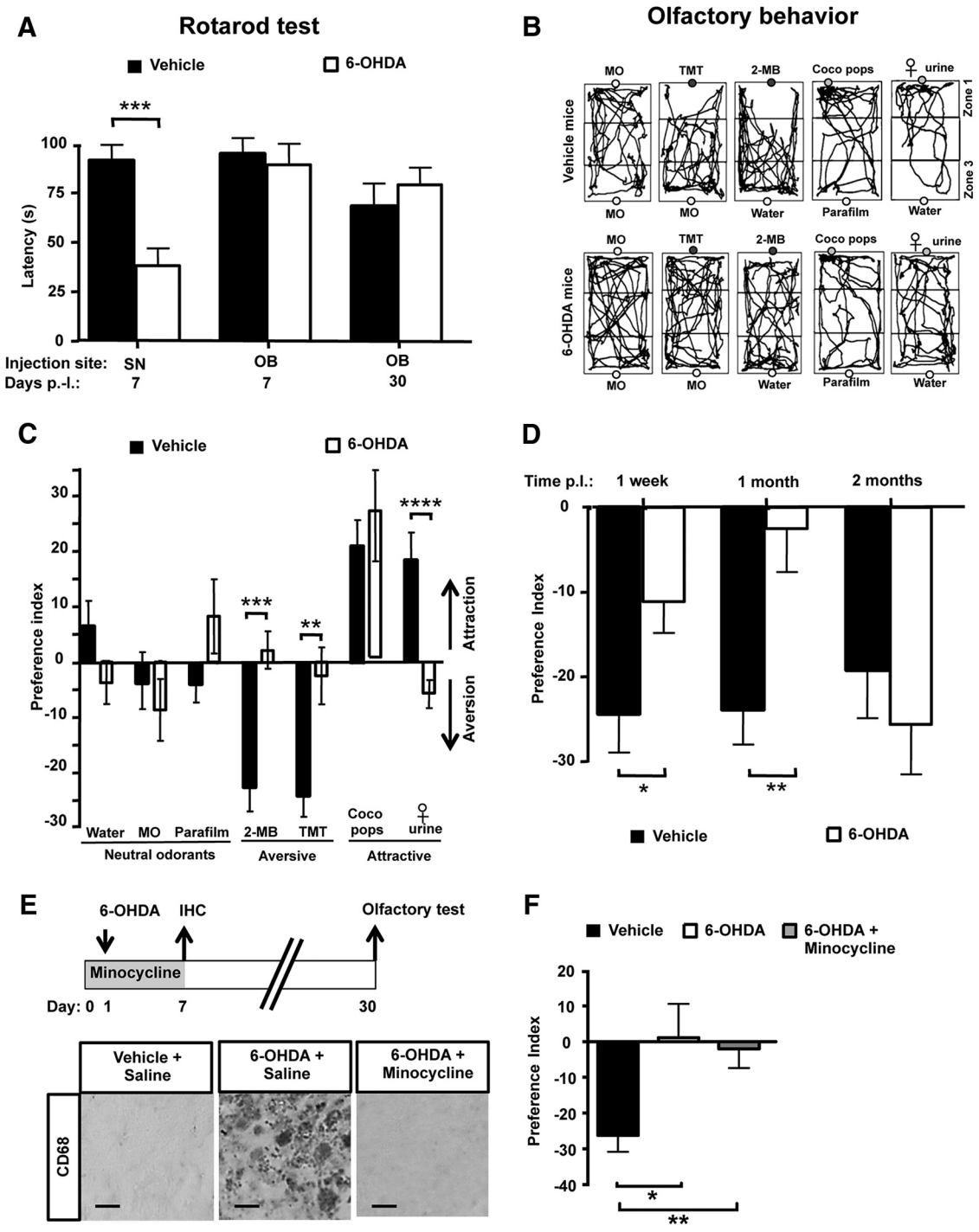

Figure 5. Behavioral consequences of challenging bulbar DAergic interneurons. ***A***, Mean latency before falling down for the rotarod test are shown for mice injected with vehicle or 6-OHDA into the right SN or the two OBs at day 7 and day 30 after lesion ($n = 8–23$ per group). Mice injected into the SN exhibited shorter latencies compared with the control groups (i.e., vehicle-injected mice and mice treated with bilateral injection of 6-OHDA into the OB), indicating motor deficits. ***B***, Representative tracing of mouse locomotion at 7 d after lesion, during a 3 min exposure to the tested odorant and to its vehicle. Panels represent the third stage of one session of the innate olfactory test habituation: exposure to the tested odorant in zone 1 and to its vehicle in zone 3. Top, Tracings of a vehicle-injected mouse ("vehicle mice"). Bottom, Tracings of a 6-OHDA-injected mouse ("6-OHDA mice"). The position of the mouse was quantified in the cage test by measuring the time spent in zone 1 and zone 3. The tested odorants were MO, TMT, 2-MB acid, Coco Pop cereals, and pool of female urines ("female urine"). Vehicle odorants were MO, water, or Parafilm as appropriate. Odorants were positioned in the middle of zone 1, except for Coco Pop cereals, which were exposed in the left part of zone 1. Whereas vehicle mice avoid aversive olfactory cues (TMT and 2-MB acid), 6-OHDA-treated mice showed no interest in these odorants. Moreover, whereas female urine attracted the vehicle mice, the 6-OHDA mice showed no interest to this social scent. ***C***, Preference index values for mice injected into the two OBs by vehicle (black columns) or 6-OHDA (white columns) at 7 d after lesion ($n = 14–20$ mice per group, per odorants). Olfactory cues were chosen to be neutral (water, MO, Parafilm), aversive (2-MB acid, TMT), or attractive (Coco Pop cereals, female urine). Preference index = time spent in zone 1 during odorant trial − time spent in zone 1 during vehicle trial. Positive values indicate attraction and negative value repulsion. Female urine was strongly attractive for vehicle male mice but not for 6-OHDA-injected mice. 2-MB acid and TMT elicited robust aversion for vehicle mice, but not for 6-OHDA-injected mice. ***D***, Preference index values for mice injected into the two OBs by vehicle (black) or 6-OHDA (white) at 1 week, 1 month, and 2 months after lesion ($n = 15–18$ mice per group). The tested odorant is the aversive odorant TMT. Whereas TMT induces a strong avoidance for vehicle mice, the response to this olfactory cue was altered in 6-OHDA-treated mice but restored at 2 months after lesion. ***E***, Minocycline treatment blocks the strong neuroinflammation induced by 6-OHDA lesion. Top, Design of the experimental procedure. Minocycline or saline was administered during 8 d, starting 1 d before 6-OHDA lesion of the OB. A 6-OHDA-containing solution, or vehicle alone, was infused into the (*Figure legend continues.*)

$p = 0.0068$; day 7 after lesion, $t_{(31)} = 2.192$, $p = 0.0360$; 1 month after lesion, $t_{(30)} = 3.240$, $p = 0.0029$). However, the TMT-induced response recovered 2 months after the 6-OHDA lesion, a time window necessary for inflammation resolution and a total recovery of the DAergic cell population in the dorsal OB (Fig. 1*F*). It could be argued that olfactory alteration and its recovery might result from the strong transient inflammation of the OB induced by 6-OHDA treatment. To test this possibility, mice received an anti-inflammatory drug, minocycline, to inhibit microglial activation (Fig. 5*E*). We found that, 7 d after 6-OHDA lesion of the OB, minocycline treatment strongly reduced CD68 immunoreactivity, indicating reduced neuroinflammation (Fig. 5*E*). However, we found that minocycline treatment did not prevent the massive loss of TH^+ bulbar cells 7 d after 6-OHDA lesioning (comparison between controls, lesioned, and minocycline-treated and lesioned mice, $F_{(2,6)} = 2.34$, $p = 0.1774$). We then investigated whether minocycline treatment is able to restore olfaction after 6-OHDA lesion (Fig. 5*F*). No difference was found in the preference index in the TMT innate olfactory test between lesioned mice and minocycline-treated lesioned mice (Fig. 5*F*). These findings indicate that minocycline efficiently prevents microglial activation in response to the lesion without reducing the lesion itself and that inflammation is not involved in 6-OHDA-induced olfactory impairments.

Discussion

The present study reports, for the first time, that 6-OHDA lesioning of the dorsal OB results in the following: (1) a transient selective ablation followed by a full recovery of DAergic interneurons in the injected zone; and (2) a transient impairment of olfactory-guided innate behaviors that depend on both social and nonsocial olfactory cues, followed by a full recovery. These findings confirm and extend previous work showing the importance of the dorsal portion of the OB in olfactory information processing that underlies some olfactory-driven behaviors (Kobayakawa et al., 2007; Dewan et al., 2013).

Injection of 6-OHDA induces a local depletion of DAergic cells

To develop a model of PD, numerous studies have used 6-OHDA-induced lesion of the nigrostriatal system (Sotelo et al., 1973; Andrew et al., 1993; Tieu, 2011). We found that injecting 6-OHDA into the OB induces a transient loss of DAergic interneurons, leading to a reversible impairment of olfaction. This finding underscores the importance of DA for the sense of smell, in addition to its crucial known roles in the planning of movements, mood, and motivation.

Similar to our work, previous studies have shown that OB DAergic interneurons are crucial for sensory information processing and olfactory abilities, such as perception, discrimination, and olfactory social interactions (Doty and Risser, 1989; Sallaz and Jourdan, 1992; Hsia et al., 1999; Murphy et al., 2005; Serguera et al., 2008; Escanilla et al., 2009; Prediger et al., 2009). DA is directly involved in the presynaptic inhibition of olfactory sensory neurons, and it modulates interglomerular connectivity, thus contributing to the unique proposed functions of TH-containing cells among other types of PGN in odorant detection threshold and odorant discrimination ability. Consistent with this, individuals with PD showing characteristically altered DA function also exhibit impairment of olfactory performance (Ansari and Johnson, 1975; Höglinger et al., 2004; Meusel et al., 2010).

Previous work on rodents indicated that DAergic cell ablation and olfactory deficits can also be achieved with a variety of neurotoxins, including the most commonly used MPTP. However, their cytotoxic effects, independent of the site of administration, extend to the whole brain, including the nigrostriatal pathway and the SVZ, thus bringing confounded results (Höglinger et al., 2004; Jackson-Lewis and Przedborsky, 2007; Tieu, 2011). Here we chose 6-OHDA to target DAergic neurons in only the dorsal part of the OB and to bypass the blood–brain barrier. We found that 6-OHDA injection only produces a local neurotoxic effect in the dorsal GL where it eliminates DAergic cells located in the injected area but spares other DAergic cells located in noninjected OB and other brain areas. Mice bilaterally injected with 6-OHDA into the OB have an unchanged performance in the rotarod test, indicating that the injected neurotoxin did not retrogradely diffuse to brain centers involved in locomotor activities and behaviors (e.g., nigrostriatal pathway). The number of DA PGNs that survive in the lesioned GL is ~50% at day 7 after lesioning despite the very high dose we used that kills almost all DA neurons in the SN. Interestingly another neurotoxin MPTP also leaves many DA PGN survivors, whereas DA neurons of the SN are strongly affected (Prediger et al., 2009). These observations are similar to the relative protection against neurotoxicity in ventral tegmental area cells compared with SN cells. They bring new insights in understanding potential neuroprotective mechanisms, such as the expression levels of the DA transporter and/or responses to oxydative stress.

Several studies have reported that 6-OHDA induces microglial activation that may be deleterious for DAergic cells (Akiyama and McGeer, 1989; He et al., 2001; Virgone-Carlotta et al., 2013). We confirm that 6-OHDA can induce strong microglial activation that occurs only locally in the injected area without affecting the rest of the bulb, including the DAergic cells located outside of the injected area. Herein, we demonstrated that an anti-inflammatory treatment, minocycline, blocks the strong neuroinflammation induced by 6-OHDA lesion but did not restore the altered olfactory response to TMT, thus suggesting that chemical-induced olfactory impairment does not result from inflammation.

Adult neurogenesis rescues DAergic cell loss in the OB

In rodents, the functional relevance of the constitutive adult neurogenesis in the healthy brain is beginning to be unraveled, ranging from perceptive to cognitive functions, including learning and memory, mood regulation, pattern separation, and behavioral responses to olfactory cues (Lazarini and Lledo, 2011; Sakamoto et al., 2011; Alonso et al., 2012; Freund et al., 2013). Reactive adult neurogenesis might be involved in the natural self-repair processes to injury (Cave et al., 2014). We present evidence that adult neurogenesis provides the OB with new DAergic neurons to replace the cell loss. First, we found that the number of DCX-positive immature neurons increases in the lesioned OB, but not elsewhere. Using lentiviral labeling of RMS-migrating neuroblasts, we showed that a significant proportion of new neurons in the lesioned OB originate from the SVZ. Another poten-

←

(*Figure legend continued.*) dorsal part of each OB. Bottom, CD68 staining in the dorsal lesioned OB at 1 week after 6-OHDA injection in vehicle (left), 6-OHDA-lesioned (center), and minocycline-treated lesioned (right) mice. ***F***, Preference index values for mice treated with saline or minocycline (gray) for 1 week and injected at day 1 into the two OBs by vehicle (black) or 6-OHDA (white) at 1 month after lesion ($n = 7$–10 mice per group). The response to TMT is unchanged by minocycline treatment. *$p < 0.05$. **$p < 0.01$. ***$p < 0.001$. ****$p < 0.0001$. Scale bar, 10 μm.

tial source for neuronal replacement in the lesioned bulb is an *in situ* generation from local neuronal progenitors. Although we did not find any evidence supporting *in situ* proliferation of DCX-expressing neuroblasts, or Olig2-expressing neural progenitors, after 6-OHDA injection, we cannot rule out the possibility that new DAergic interneurons originated from other yet nonidentified neuronal progenitors.

The increased incorporation of adult-generated neurons into the lesioned GL probably reflects an increased survival of adult-born TH^+ cells in the infused area because cell proliferation in the SVZ and RMS remains constant. This effect seems to be specific to PGNs because the number of new neurons in the GCL was unchanged after 6-OHDA lesioning. This effect is reminiscent of data showing that, after standard DAergic denervation, general SVZ neurogenesis decreases but DAergic neuronal production in the OB increases (Sui et al., 2012).

The nature of the putative "integration" signal remains unknown. It is possible that developmental signals and synaptic contacts established by sensory neurons enhance the integration of new neurons into the lesioned OB circuits and may specify DAergic phenotypes (Brill et al., 2008; Ninkovic et al., 2010; Banerjee et al., 2013; Bergami et al., 2013). Interestingly, the survival of new OB interneurons is also increased in mouse models where adult SVZ neurogenesis has been partially disrupted, thus indicating the inverse relationship that links the quantities of recruited neurons with their survival (Winner et al., 2006; Lazarini et al., 2009; Sui et al., 2012).

Similar to the present study, recent findings have shown that new neurons can compensate for depleted neuronal GC and PGN subsets in the OB (Yamada et al., 2004; Liu and Guthrie, 2011; Murata et al., 2011; Sawada et al., 2011). Selective DAergic cell generation was noted in OB 1 week after DA depletion induced by MPTP (Yamada et al., 2004). Our data, together with previous studies, indicate that adult neurogenesis is required for maintaining OB circuits and replacing DAergic cells essential to olfactory processing.

A role for adult DAergic neurogenesis in restoring innate olfactory responses

The transient impairment of olfactory-induced behaviors seen after 6-OHDA injection is consistent with previous studies showing olfactory impairment and recovery after MPTP DAergic depletion (Höglinger et al., 2004; Tieu, 2011). The spontaneous recovery after toxin-induced DAergic cell death is very similar to the motor behavioral recovery seen in 6-OHDA- and MPTP-lesioned rodents and primates (Fisher et al., 2004; Petzinger et al., 2006; Golden et al., 2013). Motor recovery occurs in these cases after structural remodeling, including sprouting of surviving DAergic cells (Petzinger et al., 2013). We propose that adult neurogenesis represents another means by which functional circuits could be restored without discarding other potential mechanisms. It is important to note that we observed a complete recovery of the number of TH^+ cells at 1 month after 6-OHDA lesion, whereas a full behavioral recovery was seen 2 months later. This delay may reflect a mismatch between the mere neuronal recruitment (4 weeks) and their functional maturation (4–8 weeks). Such discrepancy has been already reported in studies showing that adult-born hippocampal neurons contribute to behavior only when reaching the age of 4–6 weeks (Denny et al., 2012). In our context, one could hypothesize that neurons need to establish a certain number of functional synapses in order for behavior to be restored after 6-OHDA lesion, and this might occur after 4 weeks. Further experiments aiming at assessing firing activity, synapse formation, dendritic complexity, dendritic dynamics, or axonal growth are required to unequivocally disambiguate the mismatch between TH^+ cell number and behavioral recovery.

Our data indicate that a 6-OHDA lesion to the dorsal OB impairs innate behaviors triggered by nonsocial and social odorant cues. This finding highlight the importance of the dorsal OB for sensory information processing of innate responses and is consistent with previous studies reporting altered olfactory responses to predator odorants, spoiled smells, and conspecific odors, after genetic depletion of the OB dorsal zone (Kobayakawa et al., 2007; Dewan et al., 2013). The present study points out a key role for dopamine signaling in supporting innate olfactory-driven behaviors and the restorative functions of adult OB neurogenesis.

References

Adam Y, Mizrahi A (2010) Circuit formation and maintenance: perspectives from the mammalian olfactory bulb. Curr Opin Neurobiol 20:134–140. CrossRef Medline

Adam Y, Mizrahi A (2011) Long-term imaging reveals dynamic changes in the neuronal composition of the glomerular layer. J Neurosci 31:7967–7973. CrossRef Medline

Akiyama H, McGeer PL (1989) Microglial response to 6-hydroxydopamine-induced substantia nigra lesions. Brain Res 489:247–253. CrossRef Medline

Alonso M, Lepousez G, Sebastien W, Bardy C, Gabellec MM, Torquet N, Lledo PM (2012) Activation of adult-born neurons facilitates learning and memory. Nat Neurosci 15:897–904. CrossRef Medline

Alvarez-Buylla A, Lim DA (2004) For the long run: maintaining germinal niches in the adult brain. Neuron 41:683–686. CrossRef Medline

Andrew R, Watson DG, Best SA, Midgley JM, Wenlong H, Petty RK (1993) The determination of hydroxydopamines and other trace amines in the urine of parkinsonian patients and normal controls. Neurochem Res 18:1175–1177. CrossRef Medline

Ansari KA, Johnson A (1975) Olfactory function in patients with Parkinson's disease. J Chronic Dis 28:493–497. CrossRef Medline

Baker H, Kawano T, Margolis FL, Joh TH (1983) Transneuronal regulation of tyrosine hydroxylase expression in olfactory bulb of mouse and rat. J Neurosci 3:69–78. Medline

Banerjee K, Akiba Y, Baker H, Cave JW (2013) Epigenetic control of neurotransmitter expression in olfactory bulb interneurons. Int J Dev Neurosci 31:415–423. CrossRef Medline

Bergami M, Vignoli B, Motori E, Pifferi S, Zuccaro E, Menini A, Canossa M (2013) TrkB signaling directs the incorporation of newly generated periglomerular cells in the adult olfactory bulb. J Neurosci 33:11464–11478. CrossRef Medline

Borisovska M, Bensen AL, Chong G, Westbrook GL (2013) Distinct modes of dopamine and GABA release in a dual transmitter neuron. J Neurosci 33:1790–1796. CrossRef Medline

Brill MS, Snapyan M, Wohlfrom H, Ninkovic J, Jawerka M, Mastick GS, Ashery-Padan R, Saghatelyan A, Berninger B, Götz M (2008) A dlx2- and pax6-dependent transcriptional code for periglomerular neuron specification in the adult olfactory bulb. J Neurosci 28:6439–6452. CrossRef Medline

Brown JP, Couillard-Després S, Cooper-Kuhn CM, Winkler J, Aigner L, Kuhn HG (2003) Transient expression of doublecortin during adult neurogenesis. J Comp Neurol 467:1–10. CrossRef Medline

Carleton A, Petreanu LT, Lansford R, Alvarez-Buylla A, Lledo PM (2003) Becoming a new neuron in the adult olfactory bulb. Nat Neurosci 6:507–518. CrossRef Medline

Cave JW, Wang M, Baker H (2014) Adult subventricular zone neural stem cells as a potential source of dopaminergic replacement neurons. Front Neurosci 8:16. CrossRef Medline

de Chaumont F, Dallongeville S, Chenouard N, Hervé N, Pop S, Provoost T, Meas-Yedid V, Pankajakshan P, Lecomte T, Le Montagner Y, Lagache T, Dufour A, Olivo-Marin JC (2012) Icy: an open bioimage informatics platform for extended reproducible research. Nat Methods 9:690–696. CrossRef Medline

Denny CA, Burghardt NS, Schachter DM, Hen R, Drew MR (2012) 4- to 6-week-old adult-born hippocampal neurons influence novelty-evoked

exploration and contextual fear conditioning. Hippocampus 22:1188–1201. CrossRef Medline

Dewan A, Pacifico R, Zhan R, Rinberg D, Bozza T (2013) Non-redundant coding of aversive odours in the main olfactory pathway. Nature 497:486–489. CrossRef Medline

Doty RL, Risser JM (1989) Influence of the D-2 dopamine receptor agonist quinpirole on the odor detection performance of rats before and after spiperone administration. Psychopharmacology (Berl) 98:310–315. CrossRef Medline

Du Y, Ma Z, Lin S, Dodel RC, Gao F, Bales KR, Triarhou LC, Chernet E, Perry KW, Nelson DL, Luecke S, Phebus LA, Bymaster FP, Paul SM (2001) Minocycline prevents nigrostriatal dopaminergic neurodegeneration in the MPTP model of Parkinson's disease. Proc Natl Acad Sci U S A 98:14669–14674. CrossRef Medline

Escanilla O, Yuhas C, Marzan D, Linster C (2009) Dopaminergic modulation of olfactory bulb processing affects odor discrimination learning in rats. Behav Neurosci 123:828–833. CrossRef Medline

Feierstein CE, Lazarini F, Wagner S, Gabellec MM, de Chaumont F, Olivo-Marin JC, Boussin FD, Lledo PM, Gheusi G (2010) Disruption of adult neurogenesis in the olfactory bulb affects social interaction but not maternal behavior. Front Behav Neurosci 4:176. CrossRef Medline

Fisher BE, Petzinger GM, Nixon K, Hogg E, Bremmer S, Meshul CK, Jakowec MW (2004) Exercise-induced behavioral recovery and neuroplasticity in the 1-methyl-4-phenyl-1,2,3,6-tetrahydropyridine-lesioned mouse basal ganglia. J Neurosci Res 77:378–390. CrossRef Medline

Freund J, Brandmaier AM, Lewejohann L, Kirste I, Kritzler M, Krüger A, Sachser N, Lindenberger U, Kempermann G (2013) Emergence of individuality in genetically identical mice. Science 340:756–759. CrossRef Medline

Golden JP, Demaro JA 3rd, Knoten A, Hoshi M, Pehek E, Johnson EM Jr, Gereau RW 4th, Jain S (2013) Dopamine-dependent compensation maintains motor behavior in mice with developmental ablation of dopaminergic neurons. J Neurosci 33:17095–17107. CrossRef Medline

Halász N, Ljungdahl A, Hökfelt T, Johansson O, Goldstein M, Park D, Biberfeld P (1977) Transmitter histochemistry of the rat olfactory bulb: I. Immunohistochemical localization of monoamine synthesizing enzymes. Support for intrabulbar, periglomerular dopamine neurons. Brain Res 126:455–474. CrossRef Medline

He Y, Appel S, Le W (2001) Minocycline inhibits microglial activation and protects nigral cells after 6-hydroxydopamine injection into mouse striatum. Brain Res 909:187–193. CrossRef Medline

Höglinger GU, Rizk P, Muriel MP, Duyckaerts C, Oertel WH, Caille I, Hirsch EC (2004) Dopamine depletion impairs precursor cell proliferation in Parkinson disease. Nat Neurosci 7:726–735. CrossRef Medline

Hsia AY, Vincent JD, Lledo PM (1999) Dopamine depresses synaptic inputs into the olfactory bulb. J Neurophysiol 82:1082–1085. Medline

Imayoshi I, Sakamoto M, Ohtsuka T, Takao K, Miyakawa T, Yamaguchi M, Mori K, Ikeda T, Itohara S, Kageyama R (2008) Roles of continuous neurogenesis in the structural and functional integrity of the adult forebrain. Nat Neurosci 11:1153–1161. CrossRef Medline

Jablonska B, Aguirre A, Raymond M, Szabo G, Kitabatake Y, Sailor KA, Ming GL, Song H, Gallo V (2010) Chordin-induced lineage plasticity of adult SVZ neuroblasts after demyelination. Nat Neurosci 13:541–550. CrossRef Medline

Jackson-Lewis V, Przedborski S (2007) Protocol for the MPTP mouse model of Parkinson's disease. Nat Protoc 2:141–151. CrossRef Medline

Kiyokage E, Pan YZ, Shao Z, Kobayashi K, Szabo G, Yanagawa Y, Obata K, Okano H, Toida K, Puche AC, Shipley MT (2010) Molecular identity of periglomerular and short axon cells. J Neurosci 30:1185–1196. CrossRef Medline

Kobayakawa K, Kobayakawa R, Matsumoto H, Oka Y, Imai T, Ikawa M, Okabe M, Ikeda T, Itohara S, Kikusui T, Mori K, Sakano H (2007) Innate versus learned odour processing in the mouse olfactory bulb. Nature 450:503–508. CrossRef Medline

Kohwi M, Osumi N, Rubenstein JL, Alvarez-Buylla A (2005) Pax6 is required for making specific subpopulations of granule and periglomerular neurons in the olfactory bulb. J Neurosci 25:6997–7003. CrossRef Medline

Kosaka T, Kosaka K (2008) Tyrosine hydroxylase-positive GABAergic juxtaglomerular neurons are the main source of the interglomerular connections in the mouse main olfactory bulb. Neurosci Res 60:349–354. CrossRef Medline

Kosaka T, Kosaka K (2012) Further characterization of the juxtaglomerular neurons in the mouse main olfactory bulb by transcription factors, Sp8 and Tbx21. Neurosci Res 73:24–31. CrossRef Medline

Lagace DC, Whitman MC, Noonan MA, Ables JL, DeCarolis NA, Arguello AA, Donovan MH, Fischer SJ, Farnbauch LA, Beech RD, DiLeone RJ, Greer CA, Mandyam CD, Eisch AJ (2007) Dynamic contribution of nestin-expressing stem cells to adult neurogenesis. J Neurosci 27:12623–12629. CrossRef Medline

Lazarini F, Lledo PM (2011) Is adult neurogenesis essential for olfaction? Trends Neurosci 34:20–30. CrossRef Medline

Lazarini F, Mouthon MA, Gheusi G, de Chaumont F, Olivo-Marin JC, Lamarque S, Abrous DN, Boussin FD, Lledo PM (2009) Cellular and behavioral effects of cranial irradiation of the subventricular zone in adult mice. PLoS One 4:e7017. CrossRef Medline

Lazarini F, Gabellec MM, Torquet N, Lledo PM (2012) Early activation of microglia triggers long-lasting impairment of adult neurogenesis in the olfactory bulb. J Neurosci 32:3652–3664. CrossRef Medline

Liu H, Guthrie KM (2011) Neuronal replacement in the injured olfactory bulb. Exp Neurol 228:270–282. CrossRef Medline

Liu S, Plachez C, Shao Z, Puche A, Shipley MT (2013) Olfactory bulb short axon cell release of GABA and dopamine produces a temporally biphasic inhibition-excitation response in external tufted cells. J Neurosci 33:2916–2926. CrossRef Medline

Lledo PM, Alonso M, Grubb MS (2006) Adult neurogenesis and functional plasticity in neuronal circuits. Nat Rev Neurosci 7:179–193. CrossRef Medline

Lledo PM, Merkle FT, Alvarez-Buylla A (2008) Origin and function of olfactory bulb interneuron diversity. Trends Neurosci 31:392–400. CrossRef Medline

Malkesman O, Scattoni ML, Paredes D, Tragon T, Pearson B, Shaltiel G, Chen G, Crawley JN, Manji HK (2010) The female urine sniffing test: a novel approach for assessing reward-seeking behavior in rodents. Biol Psychiatry 67:864–871. CrossRef Medline

Mejia-Gervacio S, Murray K, Sapir T, Belvindrah R, Reiner O, Lledo PM (2012) MARK2/Par-1 guides the directionality of neuroblasts migrating to the olfactory bulb. Mol Cell Neurosci 49:97–103. CrossRef Medline

Meusel T, Westermann B, Fuhr P, Hummel T, Welge-Lüssen A (2010) The course of olfactory deficits in patients with Parkinson's disease: a study based on psychophysical and electrophysiological measures. Neurosci Lett 486:166–170. CrossRef Medline

Mori K, Kishi K, Ojima H (1983) Distribution of dendrites of mitral, displaced mitral, tufted, and granule cells in the rabbit olfactory bulb. J Comp Neurol 219:339–355. CrossRef Medline

Murata K, Imai M, Nakanishi S, Watanabe D, Pastan I, Kobayashi K, Nihira T, Mochizuki H, Yamada S, Mori K, Yamaguchi M (2011) Compensation of depleted neuronal subsets by new neurons in a local area of the adult olfactory bulb. J Neurosci 31:10540–10557. CrossRef Medline

Murphy GJ, Darcy DP, Isaacson JS (2005) Intraglomerular inhibition: signaling mechanisms of an olfactory microcircuit. Nat Neurosci 8:354–364. CrossRef Medline

Ninkovic J, Mori T, Götz M (2007) Distinct modes of neuron addition in adult mouse neurogenesis. J Neurosci 27:10906–10911. CrossRef Medline

Ninkovic J, Pinto L, Petricca S, Lepier A, Sun J, Rieger MA, Schroeder T, Cvekl A, Favor J, Götz M (2010) The transcription factor Pax6 regulates survival of dopaminergic olfactory bulb neurons via crystallin αA. Neuron 68:682–694. CrossRef Medline

Nyby J, Kay E, Bean NJ, Dahinden Z, Kerchner M (1985) Male mouse attraction to airborn urinary odors of conspecific and to food odors: effects of food deprivation. J Comp Psychol 99:479–490. CrossRef

Olivo-Marin JC (2002) Extraction of spots in biological images using multiscale products. Pattern Recognition 35:1986–1996.

Pallotto M, Nissant A, Fritschy JM, Rudolph U, Sassoè-Pognetto M, Panzanelli P, Lledo PM (2012) Early formation of GABAergic synapses governs the development of adult-born neurons in the olfactory bulb. J Neurosci 32:9103–9115. CrossRef Medline

Panzanelli P, Fritschy JM, Yanagawa Y, Obata K, Sassoè-Pognetto M (2007) GABAergic phenotype of periglomerular cells in the rodent olfactory bulb. J Comp Neurol 502:990–1002. CrossRef Medline

Parrish-Aungst S, Shipley MT, Erdelyi F, Szabo G, Puche AC (2007) Quantitative analysis of neuronal diversity in the mouse olfactory bulb. J Comp Neurol 501:825–836. CrossRef Medline

Petzinger GM, Fisher B, Hogg E, Abernathy A, Arevalo P, Nixon K, Jakowec MW (2006) Behavioral motor recovery in the 1-methyl-4-phenyl-1,2,3,6-tetrahydropyridine-lesioned squirrel monkey (*Saimiri sciureus*): changes in striatal dopamine and expression of tyrosine hydroxylase and dopamine transporter proteins. J Neurosci Res 83:332–347. CrossRef Medline

Petzinger GM, Fisher BE, McEwen S, Beeler JA, Walsh JP, Jakowec MW (2013) Exercise-enhanced neuroplasticity targeting motor and cognitive circuitry in Parkinson's disease. Lancet Neurol 12:716–726. CrossRef Medline

Pignatelli A, Kobayashi K, Okano H, Belluzzi O (2005) Functional properties of dopaminergic neurones in the mouse olfactory bulb. J Physiol 564:501–514. CrossRef Medline

Pignatelli A, Borin M, Fogli Iseppe A, Gambardella C, Belluzzi O (2013) The h-current in periglomerular dopaminergic neurons of the mouse olfactory bulb. PLoS One 8:e56571. CrossRef Medline

Prediger RD, Rial D, Medeiros R, Figueiredo CP, Doty RL, Takahashi RN (2009) Risk is in the air: an intranasal MPTP (1-methyl-4-phenyl-1,2,3,6-tetrahydropyridine) rat model of Parkinson's disease. Ann N Y Acad Sci 1170:629–636. CrossRef Medline

Sakamoto M, Imayoshi I, Ohtsuka T, Yamaguchi M, Mori K, Kageyama R (2011) Continuous neurogenesis in the adult forebrain is required for innate olfactory responses. Proc Natl Acad Sci U S A 108:8479–8484. CrossRef Medline

Sallaz M, Jourdan F (1992) Apomorphine disrupts odour-induced patterns of glomerular activation in the olfactory bulb. Neuroreport 3:833–836. CrossRef Medline

Sawada M, Kaneko N, Inada H, Wake H, Kato Y, Yanagawa Y, Kobayashi K, Nemoto T, Nabekura J, Sawamoto K (2011) Sensory input regulates spatial and subtype-specific patterns of neuronal turnover in the adult olfactory bulb. J Neurosci 31:11587–11596. CrossRef Medline

Serguera C, Triaca V, Kelly-Barrett J, Banchaabouchi MA, Minichiello L (2008) Increased dopamine after mating impairs olfaction and prevents odor interference with pregnancy. Nat Neurosci 11:949–956. CrossRef Medline

Sotelo C, Javoy F, Agid Y, Glowinski J (1973) Injection of 6-hydroxydopamine in the substantia nigra of the rat: I. Morphological study. Brain Res 58:269–290. CrossRef Medline

Sui Y, Horne MK, Stanić D (2012) Reduced proliferation in the adult mouse subventricular zone increases survival of olfactory bulb interneurons. PLoS One 7:e31549. CrossRef Medline

Tan J, Savigner A, Ma M, Luo M (2010) Odor information processing by the olfactory bulb analyzed in gene-targeted mice. Neuron 65:912–926. CrossRef Medline

Tieu K (2011) A guide to neurotoxic animal models of Parkinson's disease. Cold Spring Harb Perspect Med 1:a009316. CrossRef Medline

Virgone-Carlotta A, Uhlrich J, Akram MN, Ressnikoff D, Chrétien F, Domenget C, Gherardi R, Despars G, Jurdic P, Honnorat J, Nataf S, Touret M (2013) Mapping and kinetics of microglia/neuron cell-to-cell contacts in the 6-OHDA murine model of Parkinson's disease. Glia 61:1645–1658. CrossRef Medline

Whitman MC, Greer CA (2007) Adult-generated neurons exhibit diverse developmental fates. Dev Neurobiol 67:1079–1093. CrossRef Medline

Willis GL, Singer G, Evans BK (1976) Intracranial injections of 6-OHDA: comparison of catecholamine-depleting effects of different volumes and concentrations. Pharmacol Biochem Behav 5:207–213. CrossRef Medline

Winner B, Geyer M, Couillard-Despres S, Aigner R, Bogdahn U, Aigner L, Kuhn G, Winkler J (2006) Striatal deafferentation increases dopaminergic neurogenesis in the adult olfactory bulb. Exp Neurol 197:113–121. CrossRef Medline

Wu DC, Jackson-Lewis V, Vila M, Tieu K, Teismann P, Vadseth C, Choi DK, Ischiropoulos H, Przedborski S (2002) Blockade of microglial activation is neuroprotective in the 1-methyl-4-phenyl-1,2,3,6-tetrahydropyridine mouse model of Parkinson disease. J Neurosci 22:1763–1771. Medline

Yamada M, Onodera M, Mizuno Y, Mochizuki H (2004) Neurogenesis in olfactory bulb identified by retroviral labeling in normal and 1-methyl-4-phenyl-1,2,3,6-tetrahydropyridine-treated adult mice. Neuroscience 124:173–181. CrossRef Medline

Zhou Q, Anderson DJ (2002) The bHLH transcription factors OLIG2 and OLIG1 couple neuronal and glial subtype specification. Cell 109:61–73. CrossRef Medline